Eliminating perspective Elongation for LGS based AO-systems at ELTs

Stephan Kellner*[a, b], Roberto Ragazzoni[c], Emiliano Diolaiti[d], Wolfgang Gaessler[a], Jacopo Farinato[c]

[a]Max Planck Institut fuer Astronomie, Koenigstuhl 17, 69117 Heidelberg, Germany;
[b]W.M. Keck Observatory, 65-1120 Mamalahoa Hwy, Kamuela, 96743, Hawaii, USA
[c]INAF -Astronomical Observatory of Padova, Vicolo dell'Osservatorio 5, 35122 Padova -Italy
[d]Osservatorio Astronomico di Bologna via Ranzani, 1 - 40127 Bologna - Italy

ABSTRACT

Laser Guide Star Adaptive Optics systems become in the moment reality at several 8…10m class telescope facilities. At these aperture diameters all effects, arising from the finite distance and vertical extend of the artificial excited guide star can still be neglected for the wavefront sensing process. This is changing completely when the telescope diameter become further increased as it is the case of next generation Extremely Large Telescopes. Effects such as perspective elongation become dominant and impact negatively the wavefront sensing process. This will result in severe quality restrictions for next generation Adaptive Optics systems. In this paper we want to introduce and explain in detail a novel kind of wavefront sensing techniques, optimized to overcome perspective elongation. Its basic idea is to project the generated LGS virtually to infinity. We will give a theoretical introduction and some background information about the proposed sensing concept and introduce a practical solution for a potential optical setup. The latter is based on inverting the so called Bessel Beam concept, producing diffraction less beam over a certain finite range. Furthermore we will characterize the new sensor type, compare the senor efficiency to alternative approaches and discuss finally both its advantages and disadvantages.

Keywords: Adaptive Optics, wavefront sensing, Extremely Large Telescopes

1. INTRODUCTION

In order to provide astronomical instruments with almost flat wave fronts in real time, natural guide star adaptive optics system are already integrated in most mid- to large sized telescopes facilities world wide. Although such systems deliver remarkable scientific results, their limited sky coverage is still a major issue. Such constraints arise due to a combination of required guide star brightness and constraints on its allowed distance to the scientific target. Artificial guide stars, generated in the mesosphere by means of high power sodium lasers, seem to have promising capability to increase drastically the sky-coverage. Therefore, all 8…10m class telescope facilities are or become upgraded with such laser systems (Wizinowich et al. (2006)) producing already first scientific results. As pointed out by several author, also for Extremely Large Telescopes (ELT) (Gilmozzi et al. (1998), Mountain et al. (1997)) (multiple) LGS will be an essential premise to reach their full potential. However a simple scaling of a current sodium-AO-system to dimensions of ELTs leads to several drawbacks which will impact the system design in several ways. For instance the dimensions of the primary optics combined with the finite distance and vertical extend of the sodium layer will limit the wave front sensing capability for currently operated wave front sensor types, since the sensor has to deal with an extended lights source located at a finite distance. In this framework perspective elongation will be - besides several further issues which have been described elsewhere (Ragazzoni et al. (2006)) – the major error source in determining atmospherical wavefront aberrations. In the case of a Shack-Hartmann-Sensor (SHS), perspective elongation will lead to imaged spot sizes on the detector of up 6" for D=60m telescope. Moreover centroiding algorithms will be further limited by the radial dependence of the spot shape. The latter tends to be more elliptically for sub apertures close the edge of the telescope even in the case of an on-axis laser launch. To counteract these problems, several mainly technically based approaches are currently under investigation. However, their practical realization turns out to be very challenging. One approach is "Temporal gating", a techniques where a shutter at the CCD is synchronized to short laser pulses. It would limit the resulting spot

Advances in Adaptive Optics II, edited by Brent L. Ellerbroek, Domenico Bonaccini Calia,
Proc. of SPIE Vol. 6272, 62725E, (2006) · 0277-786X/06/$15 · doi: 10.1117/12.671029

sizes at the WFS to the order of the seeing at the cost of light efficiency. Temporal gating might be optimized by introducing dynamical refocusing (Lloyd-Hart et al. (2005), Beckers et al. (2004)), which increases on the other hand the further the complexity of the Adaptive Optics system.

We, however, want to follow a different approach by introducing novel wavefront sensing concepts. All those ideas are optimized to match the given telescope-LGS geometry in a more natural way. One concept - based a reflected rod - has been introduced recently. Its functionality has already been proven in both static and dynamic open loop experiments performed in the lab and on-sky. As a major disadvantage and imposed due to the radial symmetry of the sensor, this method is lacking in information on the wavefront error in radial direction. In this paper we want to discuss in more detail a further wavefront sensor type, which is able to sense the incoming wavefront in radial direction. The sensing method is based on the idea of inverting the known Bessel Beam concept. Incoming light is treated as to be from an infinite distant source and all effects related to perspective elongation can in this way ruled out, as we will show now.

2. CREATING BESSEL BEAMS

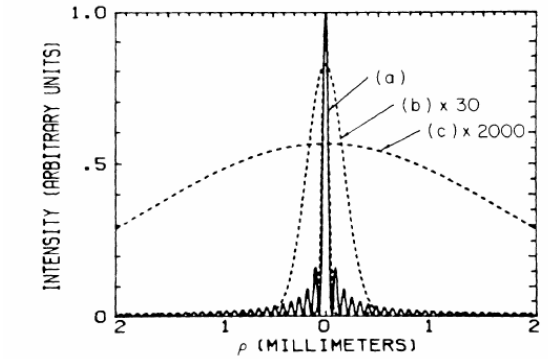

Figure 1: Comparison of transverse beam profile of a Bessel Beam and a Gaussian Beam of the same spot size propagating along the z-axis. The Bessel Beam profile (solid line) is invariant along the axis of propagation. (Images are taken from Durnin et al. (1987))

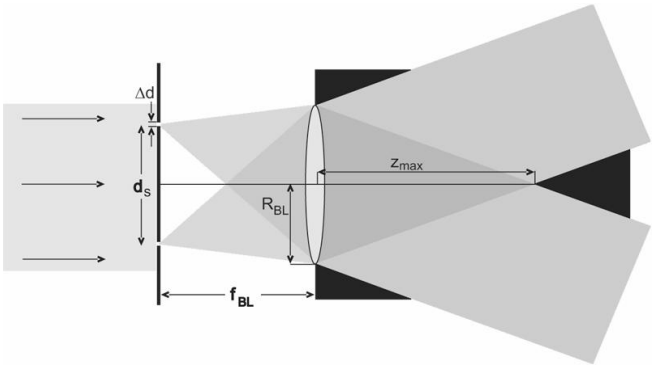

Figure 2: Arrangement to create a non diffractive beam. Collimated light is sent through a circular slit mask in the focal plane. Behind the lens, the light will form a beam a long the optical axis, which does nor diffract.

Bessel Beams are a concept to create diffraction-less beams over a certain range in the propagation direction of the light wave. Any beam with the intensity maximum along the axis of propagation is undergoing diffractive spreading proportional to the ratio of the wavelength λ over the beam size r. This leads to a rapid decrease of the on-axis intensity in the direction of propagation (see Figure 1). The spreading is determined initially by the nature of electromagnetic waves and gets increasingly noticeable at the distance r^2/λ, which is called the Rayleigh range. Techniques to reduce diffractive spreading have been pursued for a long time, for example to design super gain antennas (Francia et al. (1952)). In Durnin et al. (1987) solutions in free space to the Helmholtz wave equation

$$[\nabla^2 + \kappa^2]\Phi(r,\kappa) = 0 \qquad (1)$$

are shown, which are non-diffractive over a finite distance without violating the law of diffraction. The simplest of Durnin's predicted non-spreading beam solutions, which satisfy equation (1), is a monochromatic wave, propagating in the z-direction with a field-amplitude of

$$\Phi(x,y,z,\kappa) = \exp(i\beta z)J_0(\alpha,\rho) \qquad (2)$$

where $\alpha^2+\beta^2 = \kappa^2$, $x^2 + y^2 = \rho^2$and J_0 is the zero-order Bessel function. The half-width of the central peak is approximately given by α while the envelope of the Bessel function decays as ρ^{-1}. These classes of solutions obviously have an intensity distribution in the x-y plane denoted by the zero-order Bessel function. Hence these kinds of beams are referred to as Bessel Beams. The theory is experimentally verified by Durnin et al. (1987) using a circular slit in the focal plane

of a lens and illuminating it from behind with collimated monochromatic light of wavelength λ. The experimental arrangement is shown in Figure 2. The lens transforms points in the focal plane, selected by a circular slit of width Δd, to plane waves of a certain direction. All these plane waves interfere along the optical axis until the end of the shadow zone z_{max}, providing within this distance a diffraction-less beam (z_{max} is determined by $R_{BL}/\tan(\vartheta)$ where ϑ is given by $\tan^{-}(d/2f_{BL})$). A variety of further possibilities exist to create Bessel Beams. Hermann et al. (1991), for instance, proposed to use conical lenses or utilize spherical aberrations.

3. THE MULTI INVERSE BESSEL BEAM SENSOR

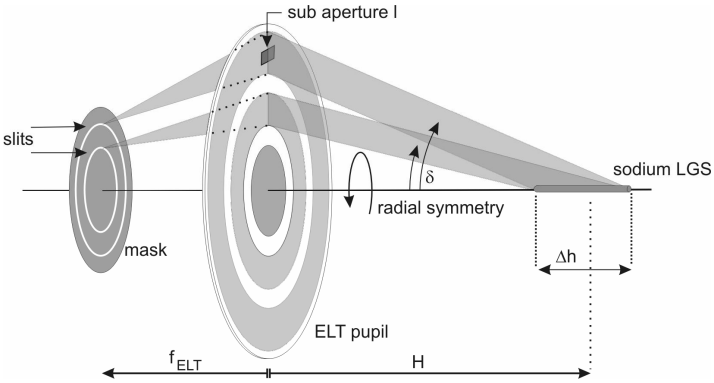

Figure 3: A mask with circular slits placed in the focal plane of the telescope selects certain angular directions of light rays originating at a LGS. This approach may be interpreted in analogy to the temporal gating approach as angular gating.

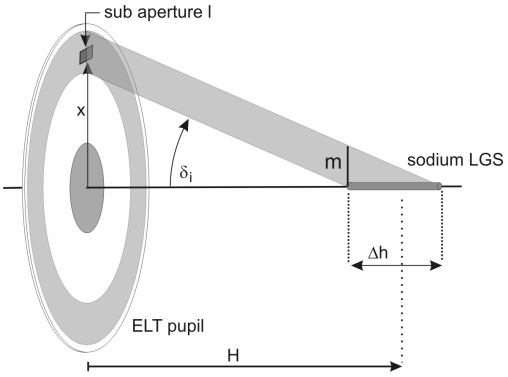

Figure 4: Geometrical condition to calculate the projected footprint size m of the LGS onto the telescope pupil.

By inverting the setup shown in Figure 2, one is able to perform wavefront sensing in the radial direction. According to the geometric optics approximation, fixed positions in the focal plane of a telescope are directly associated to directions of incoming parallel light on the sky. Therefore, a mask with circular concentric thin slits placed in the focal plane will select light rays coming from certain directions δ. This is also valid for rays originating at the LGS, which as a result is projected virtually to infinity by the mask (note: this helps to avoid geometrical effects, but the light does not sample higher layers of the atmosphere, as a true source at infinity like a star does). To deduce how the mask is able to sense an incoming wavefront of a sodium beacon, only light rays which are emitted by the LGS at a defined direction δ_i are considered. According to Figure 3, it is assumed that the sodium LGS takes shape in the mesospheric sodium layer of thickness Δh, located at a distance H from the telescope aperture. Furthermore a sub-aperture l, located at the telescope pupil in distance x from the telescope center, is considered. For the sensing process it is mandatory that the radial size of the sub-aperture has to be much smaller than the projected footprint of the LGS for the selected direction δ_i. This constraint is in the case of OWL (its foreseen central obstruction will have a diameter of 35% with respect to mirror diameter) fulfilled for any radial position of the sub-aperture, which can be revised by applying geometrical optics considerations (see Figure 4). This yields

$$\frac{x}{H - \Delta h/2} = \frac{m}{\Delta h} \tag{3}$$

an equation for m, which denotes the absolute vertical extent of the LGS footprint at the pupil. A lower limit for m is given in the case of a sub-aperture close to the edge of the central obstruction. At this point the projected footprint is still

1m and thus significantly larger than a typical sub-aperture size l (l normally is on the order of r_0, which translates in the V-band to 20 cm assuming excellent seeing conditions) in the visible .

For simplification reasons it is assumed in the following that distances between two circular slits in the focal plane have been selected such that no overlap of two successive footprints in the pupil plane occurs. In practice this means that each sub-aperture is exclusively illuminated by light from one direction δ_i; but it is important to realize that in principle the light throughput can be increased by illuminating each sub-aperture with rays from several directions. This approach leads to a new gating concept called *angular gating* (see Figure 8). Hence, in the aberration free case, the sub-aperture l will be illuminated by light of the LGS coming from portion s (see Figure 5). Introducing a wavefront distortion close to the telescope pupil, the amount of light from the LGS projected into the sub-aperture does change with the amplitude of the atmospheric phase aberration at the edges of the sub-aperture. A wavefront error with positive curvature within the sub-aperture leads to an additional amount of light refracted into the sub-aperture. Such rays are originating at additional portions s_i of the LGS and are associated with different directions than δ_i.

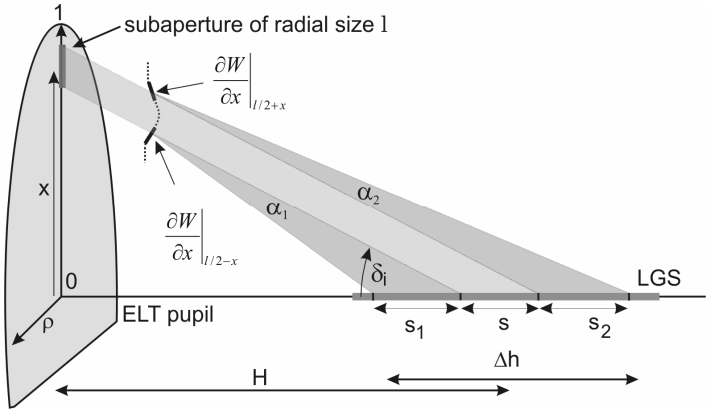

Figure 5: A radial wavefront error at the edge of the sub-aperture is related to a change of the effective beacon length illuminating the subaperture

Thus, the intensity within the sub-aperture is proportional to the "effective" length $s + s_1 + s_2$ of the beacon contributing to its illumination. By defining I and I' as brightness within the sub-aperture in the non-aberrated and aberrated case, respectively, one can describe the resulting normalized brightness fluctuation as:

$$\frac{I' - I}{I} = \frac{\Delta I}{I} \propto \frac{\Delta s}{s} = \frac{s_1 + s_2}{s} \tag{4}$$

While s is the reference beacon length for the non-aberrated case, $\Delta s = s_1 + s_2$ denotes the net change of the beacon length introduced by the radial distortion. Depending on the curvature radius, this may lead to positive or negative values for Δs and determines thus the strength of the intensity fluctuation within the sub-aperture. The maximum differential angle of a ray originating at the LGS, which will still be refracted into the sub-aperture, is related to s_i via:

$$s_i = H \frac{2H}{\rho D} \alpha_i \qquad \text{i=1,2} \tag{5}$$

Here ρ denotes the normalized radial pupil coordinate and is connected to the radial distance x from the center of the pupil via:

$$x = \frac{\rho D}{2} \tag{6}$$

The portion s in the non-aberrated case is given by:

$$s = l \frac{2H}{\rho D} \tag{7}$$

In order to compute the ratio ΔI/I, equations 4 and 5 are combined with equation 7:

$$\frac{\Delta I}{I} = \frac{H}{l}(\alpha_1 - \alpha_2) \tag{8}$$

The angle α_i is proportional to the radial wavefront slope at the edge of the sub-aperture. Therefore the difference α_1-α_2 can be written as

$$\alpha_1 - \alpha_2 = \left.\frac{\partial W(\rho,\theta)}{\partial x}\right|_{x-l/2} - \left.\frac{\partial W(\rho,\theta)}{\partial x}\right|_{x+l/2} \approx \frac{\partial^2 W(\rho,\theta)}{\partial x^2} l \tag{9}$$

leading to the second radial derivative. Moreover x has to be transformed into the normalized pupil coordinate ρ. This is done by calculating the square of the derivative $\partial x / \partial \rho$ of equation 6, which leads to an additional factor $4/D^2$:

$$\alpha_1 - \alpha_2 = \frac{\partial^2 W(\rho,\theta)}{\partial \rho^2} \frac{4}{D^2} l \tag{10}$$

By combining ultimately equations 8 and 10, one obtains a relation which describes the dependency of the normalized intensity fluctuation within the sub-aperture on the second radial derivative of the phase error of the wavefront:

$$\frac{\Delta I}{I} = \frac{4H}{D^2} \frac{\partial^2 W(\rho,\theta)}{\partial \rho^2} \tag{11}$$

It has to be pointed out that the gain $4H/D^2$ of the mask does not depend on the sub-aperture size l. The gain does not depend on any controllable parameter and is therefore fixed. In the case of 100m class telescope the factor is ~ 40. Its dependence on the distance of the guide star H might turn out to be disadvantageous, since H is a function of the telescope elevation and may vary for long exposure observations.

4. DEFINING AND CONTROLLING THE SUB-APERTURE SIZE

Still an open question is how to control the sub-aperture size, which determines the sampling accuracy of the wavefront error. The radial mask placed in the infinity focal plane influences -- depending on the phase aberrations -- the intensity distribution in the pupil plane as measured by a pupil plane WFS. The sampling grid and therefore the sub-aperture size can be adjusted by the used pixel grid of the CCD. This may be a major advantage, since its flexibility allows the system to be easily adjusted to varying atmospherical conditions.

5. EFFICIENCY ESTIMATES AND MULTIPLE GATING

The mask rejects most of the incoming light of the LGS, at first glance resulting in an inefficient usage of the available photons as in the temporal gating approach (all blocked photons can not contribute to the recorded signal). In this section both concepts will be compared in a quantitative way and it will be shown that the mask (and hence angular gating) is in terms of light efficiency superior to temporal gating. Unsolved technical issues of temporal gating are neglected. For a sub-aperture at the edge of the telescope the apparent spot elongation depends on the length of the excited column and hence in the case of temporal gating on the pulse duration τ (indicated in Figure 6 with the dashed line). As long as the angular elongation is on the order of the seeing λ/r_0, the performance of a conventional WFS will not be affected (assume for instance a SHS operated in the V-band with a sub-aperture size of the order of r_0, where each lens produces a seeing limited image of the guide star on the CCD). Therefore this constraint defines an upper limit for the effectively used beacon length for the temporal gating and hence implicitly the amount of available light. A lower limit for the slit width of the mask can be estimated by diffraction optics considerations. In this case the pupil re-imaging optics views a sub-aperture at the pupil through a thin slit of width d. Hence waves originating from each point P at the pupil have to pass the slit, which leads to diffractive spreading. This results finally in a smoothing of each single point. In order to minimize cross-talk, the induced radial smoothing of points of a sub-aperture has to be smaller than the sub-aperture size

l, which is normally adjusted to the coherence length r_0. To estimate this effect quantitatively it is assumed that each point viewed through the slit leads to a PSF, who's FWHM in the radial direction is given by λ/d. Hence one may write: $\lambda/d < l = r_0$ what finally would lead to $\lambda/r_0 < d$.

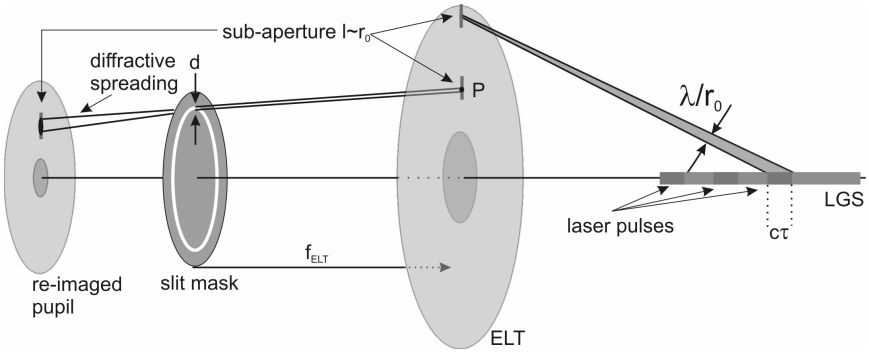

Figure 6: Efficiency comparison of slit mask and temporal gating: Temporal gating constrains the angular elongation of the LGS to the seeing λ/r_0. A lower limit for the slit width can be determined considering diffraction effects. It can be shown ultimately, that the light throughput per slit is as high as for the temporal gating.

This means that the minimum possible angular slit width in the infinity focal plane has to be of the order of the seeing. Thus the same amount of light will pass through *each slit* and enter the optical system, as in the temporal gating approach. Hence the light throughput will be identical.

To increase the throughput, one can in the first instance think about broadening the slit width. This, however, is connected with a loss of dynamic range of the sensor. A finite slit width is coupled with an additional amount of light illuminating the sub-aperture l. It originates from directions up to δ_j (see Figure 7), adjacent to direction δ_i, increasing the reference beacon length s and thus the reference intensity I. On the other hand, a given wavefront distortion will result in a fixed change of the beacon length s_i or intensity I'. For this reason the measurable net change in intensity fluctuation (= dynamic range) for a fixed wavefront distortion will decrease with increasing slit width. This has a drawback on the sensitivity of the slit mask sensing device.

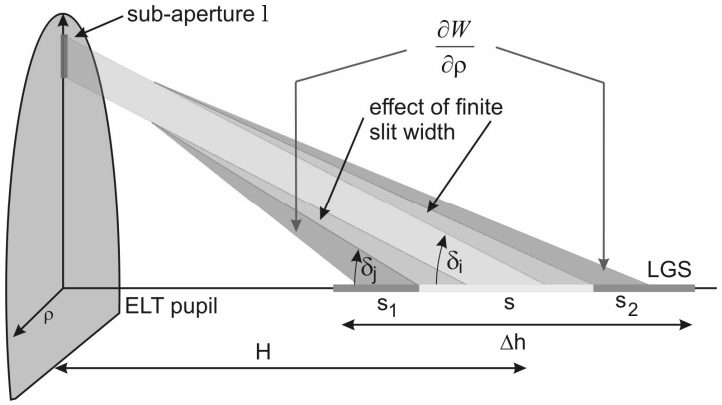

Figure 7: Consequence of broadening the slit width. Although on the one hand a gain in terms of light-throughput can be achieved, on the other hand this approach leads to a loss of dynamic range and thus sensitivity of the mask.

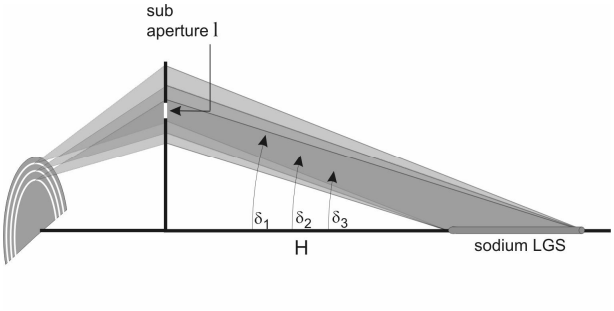

Figure 8: To increase the light throughput, a sub-aperture can be simultaneously illuminated by light from several directions *angular gating*). Depending on the radial position this leads to 4-10 times more light throughput in comparison to temporal gating.

The light selection process of the mask can be seen in analogy to the temporal gating as *angular gating*. But, unlike for temporal gating, the light throughput per sub-aperture can easily be increased performing multiple gating with multiple slits. Each sub-aperture is illuminated by light from several directions (See Figure 8), which translates simply into an increased number of concentric slits. To estimate how many different directions per sub-aperture can be used for angular gating, it is mandatory to figure out the necessary minimum distance between two successive slits. The latter is constraint, since the mask - in order to perform the sensing - has to block light within a certain differential angle (given by the expected radial wavefront distortion) around the reference direction δ_i. Otherwise, aberrated light rays which have to be blocked enter the optical system through an adjacent slit and contribute nevertheless to the intensity distribution recorded by the detector. The minimum separation between two angularly gated directions δ_i and δ_k therefore has to fulfill the condition (see Figure 9):

$$\frac{\partial W(\rho,\theta)}{\partial \rho} < \delta_i - \delta_k \qquad (12)$$

where $\partial W(\rho,\theta)/\partial\rho$ denotes the maximum radial wavefront slope which still has to be blocked. A upper limit for $\partial W(\rho,\theta)/\partial\rho$ at the edge of a sub-aperture l may be retrieved directly from the definition of r_0. The wavefront RMS phase error encircled by r_0 is 1rad = $\lambda/2\pi$. The corresponding Peak To Valley (PTV) phase fluctuations is given by deducing the typical PTV/RMS ratio. As a rule of thumb a factor 6 is used. Therefore λ is a typical upper limit for a PTV wavefront error within the sub-aperture $\lambda=r_0$. This finally translates into a maximum slope of the radial wavefront error $\partial W(\rho,\theta)/\partial\rho$ of λ / r_0. As a result, the angular distance μ between two successive slits has to be at least on the order of the seeing $\mu > \lambda/ r_0$.

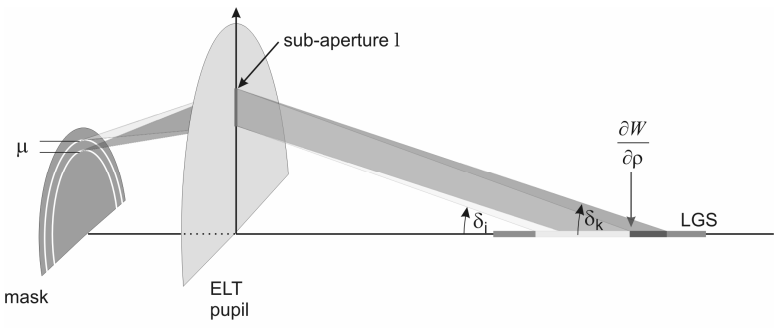

Figure 9: A condition for the minimum angular slit distance μ can be retrieved assuming that two gating directions δ_i and δ_k have to be at east separated by the expected slope of the radial wavefront error $\partial W(\rho,\theta)/\partial\rho$ at the edge of a sub-aperture .

Finally, one can derive an expression to estimate the gain of multiple angular gating with respect to temporal gating. Therefore a sub-aperture l is considered, which is located at distance ρD/2 from the center of the pupil (see Figure 10). Again ρ denotes the normalized radial pupil coordinate and D the telescope diameter. The sub-aperture will only be illuminated by light rays originating from a cone of directions located between δ_1 to δ_2, since for these directions the projected footprints of the LGS cover the sub-aperture. Using the geometrical optics approximation, M slits in the focal plane will cover an angle Mμ which is exactly the differential angle δ_2 to δ_1. M denotes a multiplicity factor describing how many slits can be used for angular gating. A relation to compute M can be deduced by realizing that the length of the absolute radial size of the LGS footprint at the pupil from direction δ_1 and the absolute length of the differential angle Mμ at the pupil are equal:

$$M = \frac{\Delta h \rho D}{2 \mu H^2} \tag{13}$$

According to equation 13, the multiplicity factor M is a function of the radial position ρ of the sub-aperture and moreover sensitive to the choice of the slit distance μ. Inserting typical numbers as for instance in the case of OWL (D=100m, μ = 1", H=100km, Delta h=10km) one obtains M ≈ 10ρ. The planned diameter of the central obstruction of OWL constrains ρ to range from 0.35 to 1. Thus the light throughput of the slit mask and therefore angular gating is at least a factor of 3.5 more efficient as temporal gating. The efficiency will benefit further from good seeing conditions, since the minimum slit-distance and slit width may be reduced.

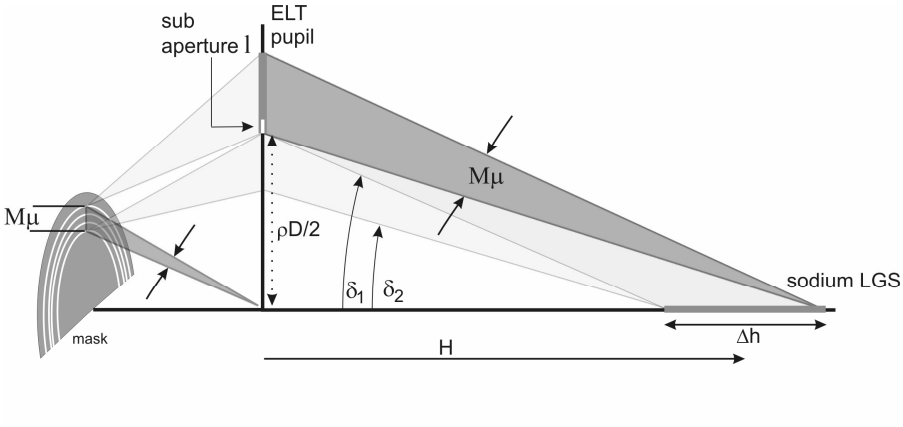

Figure 10: The achievable multiplicity factor M for multiple angular gating, and therefore the resulting gain in terms of light throughput, can be deduced following geometric optics considerations. The radial elongation of the angle Mμ at the pupil is equivalent to the projected footprint of the LGS for the direction δ_1.

5.1 Physical Extent of the Mask and Size Limitations

In the case of OWL, the physical diameter of the slit mask will have to be 0.54m (assuming a F/6 optical design for OWL, which leads to a focal length of 600m). An angular separation μ= 1" of two successive slits corresponds to a physical extent of ≈ 2.9mm in the focal plane. Assuming equidistant slits and a central obstruction of ε=0.35, the mask can be equipped with 38 slits with a width of 2.9mm. Imposed by the radial dependency of the angular gating, a choice of equidistant slits, however, would lead to a radial brightness gradient within the re-imaged pupil. Therefore a solution may be preferred where a constant gain in terms of light throughput over the pupil is guaranteed. This would correspond to a slit distance following a ρ^{-1} law. As a major limitation, the circular slit mask is, due to its radial symmetric design, only able to perform sensing in radial directions. In principle it is possible to extend the sensing capability of the mask and retrieve information about the entire wavefront phase error. One solution would be to introduce a grid of further blocking elements per slit in the azimuthal direction (on the order of the seeing). This approach is connected to a further loss of light and leads to an increasing inefficiency in terms of light throughput.

6. CONCLUSION

We presented and discussed a novel wavefront sensing concept, which is able to eliminate the effect of perspective elongation, visible at the wavefront sensor in sodium LGS based AO-systems at ELTs. The basic idea of the concept is based on considering exclusively light rays origin at points from infinity. One practical implementation of this wavefront sensing method is by inverting the so called Bessel Beam concept. A mask with circular slit is introduced as a possible sensing device. The resulting sensor is able to measure intensity fluctuations in the pupil plane, which turned out to be proportional the second radial derivative of the atmospherically induced phase errors of incoming wave fronts. The mask can in principle be combined with the z-invariant sensor leading so to a fully functional wavefront sensor. This is possible since both sensors are located at different conjugates in the image space. Due to its pupil plane sensing approach, the mask can be adapted in both, layer and star oriented wave front sensing approaches discussed in the MCAO framework.

However we finally want to point out that the concept still has to be proven in an experiment. Although the concept is in terms of light throughput at least by a factor 4-10 more efficient than the temporal gating approach, a significant amount of photons is lost by the sensing process. A disadvantage is the low flexibility of the sensor gain, since it is only a function of the distance of the guide star and the telescope diameter. The first tends to change slightly, since the height of the sodium layer may vary during observational run. The mask as sensing device is only one out of many possible practical solutions of the inverted Bessel Beams concept to project light to infinity. There may exist further more sophisticated solutions.

REFERENCES

1. Beckers J.M., et al. Proc. 2nd Workshop on Extremely Large Telescopes, Backaskog Castle, Sweden, p.123
2. Durnin J., 1987, JOSA, Vol. 4, p. 651
3. Durninj., et al., 1987, Ph.Rev. L, Vol. 58, p.1499
4. Gilmozzi R., et al. 1998, SPIE, Vol. 3352, p. 778
5. Herman R.M., et al., 1991, JOSA, Vol. 8, p.932
6. Mountain M., 1997, SPIE. Vol 2871, p. 597
7. Lyod-Hart M., et al. astro-ph 0508402
8. Ragazzoni R., et al., MNRAS 2006, accepted
9. Toraldo di Francia, 1952, Nuovo Cimento, Vol. 9, p.426